

Microfabricated torsion levers optimized for low force and high-frequency operation in fluids

Arthur Beyder*, Frederick Sachs

Department of Physiology and Biophysical Sciences, Center for Single Molecule Biophysics, State University of New York at Buffalo, 3435 Main Street, 301 Cary Hall, Buffalo, NY 14214, USA

Received 3 September 2005; accepted 30 November 2005

Abstract

We developed a mass production fabrication process for making symmetrically supported torsion cantilevers/oscillators with highly compliant springs. These torsion probes offer advantages in atomic force microscopy (AFM) because they are small, have high optical gain, do not warp and can be made with two independent axes. Compared to traditional AFM cantilevers, these probes have higher frequency response, higher Q , lower noise, better optics (since the mirror does not bend) and two data channels. Soft small levers with sub-pN force resolution can resonate cleanly above 10 kHz in water. When fabricated with a ferromagnetic coating on the rigid reflecting pad, they can be driven magnetically or serve as high-resolution magnetometers. Asymmetric levers can be tapping mode probes or high-resolution accelerometers. The dual axis gimbaled probes with two orthogonal axes can operate on a standard AFM with single beam illumination. These probes can be used as self-referencing, drift free, cantilevers where one axis senses the substrate position and the other the sample position. These levers can be optimized for differential contrast or high-resolution friction imaging.

© 2006 Elsevier B.V. All rights reserved.

PACS: 07.79.Lh; 07.79.Pk; 07.79.Sp

Keywords: Atomic force microscopes; Magnetic force microscopes; Friction force microscopes; Microfabrication; Force; Friction

1. Introduction

The atomic force microscope (AFM) has provided the ability to measure and manipulate matter at the atomic level [1]. The core of the instrument is a compliant cantilever whose bending generates the output. To first order, the bending is a linear function of the force applied by the sample. Typically, cantilever deflection is monitored by an optical lever, a laser beam reflected off the cantilever onto a position sensitive photodetector (PDT) [2].

The resolution of an AFM is limited by the physical/mechanical properties of the cantilever [3]. The scanning tip shape is convolved with the sample and thus determines the spatial resolution [4]. The force/distance resolution is limited by the thermal fluctuations of the cantilever,

$1/2k_B T$ for each degree of freedom [5]. The apparent compliance of a sample is a convolution of the compliance of the cantilever and that of the sample itself. Generally, soft cantilevers are preferred when measuring force and stiff cantilevers are preferred when measuring displacement [6].

The AFM has a particular appeal to biologists because it can be used on live samples under water, with the potential for atomic spatial resolution, examination of the forces produced by single molecules, and a time resolution approaching microseconds. However, in liquids, the cantilever behavior is significantly degraded by viscous drag [6]. Drag reduces the frequency response and the force resolution. Since the drag is a function of the object's size [7], smaller probes are better.

The first cantilevers were made from a gold foil with a diamond shard as a tip [1]. Later, silicon micromachining permitted mass production with well-defined mechanical properties [8,9]. Current commercial cantilevers are most

*Corresponding author. Tel.: +1 716 829 3289; fax: +1 716 829 2569.

E-mail address: beyder@gmail.com (A. Beyder).

URL: <http://www.sachslab.buffalo.edu>.

commonly made from silicon (Si), silicon nitride (stoichiometric— Si_3N_4 or low-stress silicon-rich—SiN) and silicon dioxide (SiO_2) [8]. The stiffness of the cantilever is a cubic function of length and an inverse cubic of thickness; high compliance (soft) levers are usually made by making levers longer [10], but long cantilevers have large surface areas, thus they are highly damped in liquid. One can also make cantilevers soft by making them thin. Crystal silicon cantilevers are generally thick ($>1\mu\text{m}$) and stiff [11]. However, using thin uniform films ($<1\mu\text{m}$) of low stress of SiN, it is possible to fabricate much softer levers [12]. All commercial cantilevers are asymmetrically supported and usually metal coated for reflectivity making them prone to warping from residual stress [13] and as a thermal bimorph, changes in temperature increase the warp [14].

To improve the cantilever response in fluid, the Hansma group made small cantilevers [15–18], as thin as 86 nm and 27 μm long [19]. However, that design had a number of practical problems. Due to their small area, there was limited access to the sample and limited target size for the optical beam. These cantilevers could not be used on standard AFMs because they required high aperture lenses to focus the beam on the cantilever [18]. Furthermore, high aperture lenses have a short working distance so that there is little room to introduce other objects such as micropipettes near the sample [20]. The small design does not resolve the general problem of continuous beam levers, that bending disperses the optical beam [21].

We have taken a different approach to making small AFM probes using symmetrically supported torsion levers. The lever itself, containing the tip, is a stiff silicon (Si) pad $\sim 20 \times 20 \times 5\mu\text{m}$ that is a convenient mirror size for standard AFM optics. The pad oscillates on compliant torsional hinges, which are made of SiN. The levers are located at the end of stiff Si extension beams that hold them away from the die, therefore increasing accessibility to the sample and optical clearance.

Torsion actuators and sensors are common mechanisms in micro-electromechanical systems (MEMS) [22–24]. Torsion oscillators are generally made from single-crystal silicon, and have served as movable mirrors, tunable capacitors, RF switches, gyroscopes and angular rate sensors [25]. Oscillators made from Si are stiff unless the fabrication is done with sub-optical resolution [22] or the beams are long [26], making them drag-prone. If the oscillators are made from softer materials, such as silicon nitride, they suffer from flexure of the entire assembly, including the support arms and the torsion pads themselves [21]. By using two different materials, the supporting structures can be stiff and the hinges soft. We developed a process to make such composite probes in a mass production environment, while retaining the flexibility to make a variety of small probes with custom geometry.

2. Methods

2.1. Device fabrication

The fabrication process can be divided into three phases: (1) a bottomside etch to produce a thin silicon membrane and to define the support chip, (2) direct fabrication of the tip, and (3) topside patterning of the stiff silicon elements and the thin film hinges. The process is summarized in Fig. 1.

We first produce the thin silicon membrane using aqueous potassium hydroxide (KOH) to etch the bottomside of $\langle 100 \rangle$ Si wafers (1a). The etch proceeds most of the way through the wafer, leaving at the topside a membrane that is stiff by comparison to the hinges. This etch step utilizes a new procedure to produce optically flat membranes of controlled thickness [27].

In the next step (1b), we deposit a SiO_2/SiN thin film stack using low-pressure chemical vapor deposition (LPCVD). We use high-quality, low-stress, silicon-rich SiN films [28]. This bottomside SiN layer is later patterned into the hinges, while the SiO_2 layer serves as protection until the final release.

The following steps are performed on the topside of the wafer to make the tips and pattern the cantilevers. Since we have SiO_2 and SiN and photoresist available for masking (2a), there are several methods available for making the tips [8,11,29,30]. Step 2b is a controlled undercut of a small masking island to produce a Si tip. We have produced high-aspect atomically sharp tips by undercutting LPCVD SiO_2 with SF_6 . We have also made lower-aspect tips using

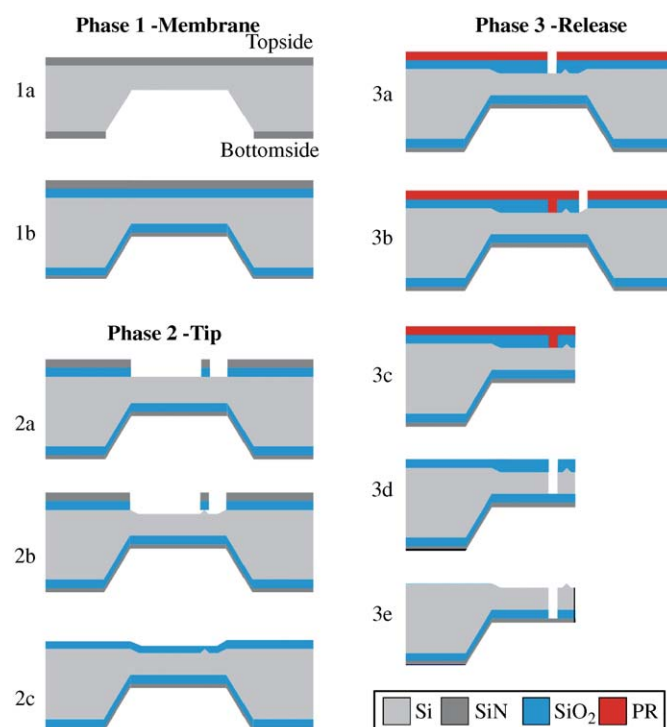


Fig. 1. Microfabrication sequence.

SiN as a mask and KOH for an anisotropic undercut. Once the tip is produced, it is protected through the rest of the process by a thin layer of plasma-enhanced chemical vapor deposited (PECVD) SiO₂ (2c).

After making the tip, we define the hinge and the oscillator. We use a double mask of PECVD silicon dioxide and photoresist to complete production of a four-level

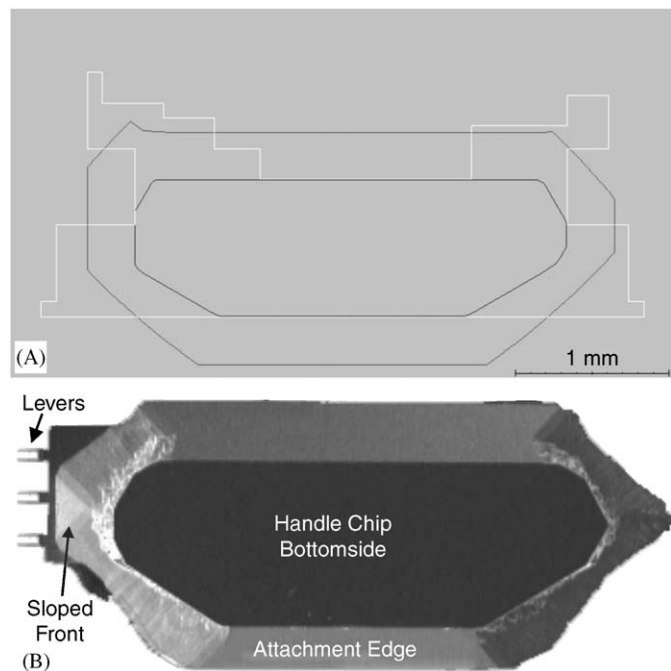


Fig. 2. (A) SIMODE simulation of the fabrication of the handle (etched in 40% KOH at 80 °C). The chip is attached to the wafer at the lower edge. (B) SEM of a fabricated handle chip.

structure. The opening for the hinges is patterned into the SiO₂ layer (3a), which is then covered by a new photoresist layer. Next, the cantilever shape is imaged onto the photoresist and etched into the silicon dioxide layer (3b). We etch the silicon around the cantilever using the inductively coupled plasma reactive ion etch (ICP-RIE) C₄H₈/SF₆ [31]. Then another RIE removes the underlying SiO₂ and SiN layers, suspending the cantilever (3c). Finally, the photoresist layer is removed, exposing the previously patterned SiO₂ layer. Again, we use ICP-RIE to release the hinges (3d). To release the nitride hinge layer and to uncover the tip, which until now has been protected by SiO₂, we selectively remove the SiO₂ using 10–50% HF (3e).

At this point, we can deposit a metal layer to increase reflectivity. The 5- μ m-thick silicon pads are reasonably reflective, but we also deposit \sim 50 nm Au to increase reflectivity [27]. We have also deposited other metals, such as Co, to produce magnetic levers for MAC mode AFM [32].

2.2. Evaluation of levers' dynamic performance

For small deflections, the lever can be treated as a simple harmonic oscillator with one degree of freedom. The oscillator is continually excited by thermal energy and this energy may be used to calibrate the oscillators' spring constants [33,34]. For calibration, we use a commercially available Quesant Nomad AFM [35]. Calibration requires two steps. In the first step, optical sensitivity of the PDT is determined by using a calibrated PZT to gently press the probe against a stiff substrate until a desired deflection is reached. This calibration is used to convert the voltage

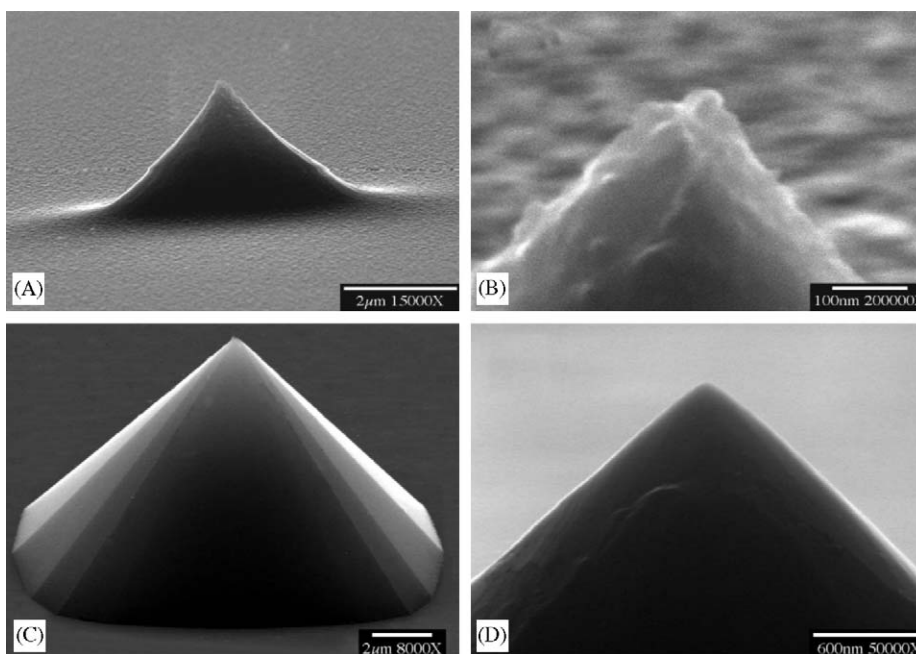


Fig. 3. SEM images of integrated tips. (A) SF₆ RIE, (B) high-magnification view of A, (C) KOH tip, (D) high-magnification view of C.

output from the PDT into z -displacement. In the second step, a time trace of the thermal noise is acquired (National Instruments A/D, PCI NIDAQ). An FFT of this data provides the power spectrum, which identifies the resonant peak of the probe. The peak is fit to a Lorentzian whose integral is the mean position noise. Thus, the value of this integral (P) provides a direct estimate of the spring constant $k = k_B T / \langle z^2 \rangle = k_B T / P$, where k_B is Boltzmann's constant and T is temperature. Once the spring constant and sensitivity are calibrated, we can measure the noise of the lever in the bandwidth of interest.

3. Results and discussion

3.1. Fabrication—features of the fabricated oscillators

3.1.1. Chip handles

We use the anisotropy of the KOH etch to produce chips that are solidly supported by the wafer throughout processing and can be easily removed from the wafer. An

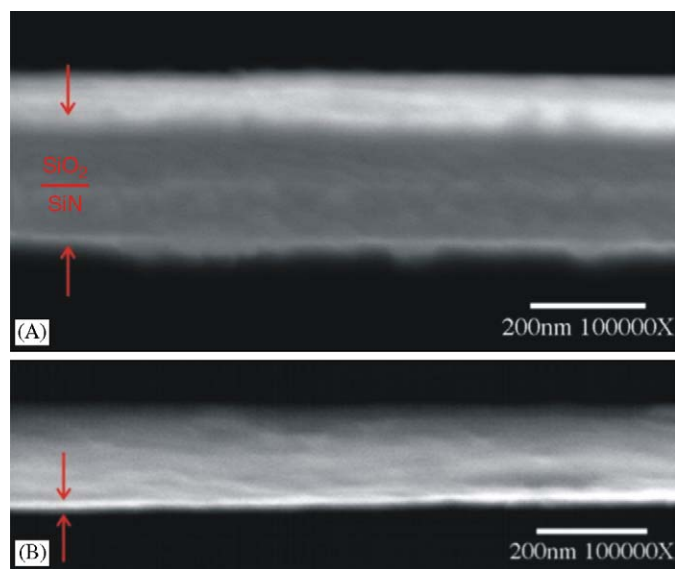


Fig. 4. (A) Hinges are produced as SiO₂/SiN stack. (B) HF may be used to produce hinges as thin as 10 nm (hinge imaged obliquely).

additional advantage of using the KOH etch to produce the chip handle is that the chip handles have a sloped front end, increasing the optical clearance (Fig. 2B). A common problem for KOH-assisted definition of silicon blocks is convex corner undercutting. During the etch, low-density, high-etch-rate Miller planes are exposed resulting in significant rounding [36,37]. This undercut is critical if the etch is deep, as is the case in the through-the-wafer etch (~450 μm) that we use. With the help of commercially available KOH etch simulation software (SIMODE, <http://www.infotech.tu-chemnitz.de/~wetel/ensimode.htm>), we were able to design a set of compensation structures at the corners that allowed production of nearly rectangular chip handles sized to fit standard AFM holders (1.8 mm × 3 mm) (Fig. 2A).

3.1.2. Silicon membranes

The Si membranes that are produced in Phase 1 are used to fabricate the tip and other stiff parts of the levers. Membranes cannot be arbitrarily thin, since the parts supporting the hinges need to be stiff and reflective, and because of its length, the extension beam is the softest. However, a typical extension beam 5 μm thick is about 1000-fold stiffer than the hinges.

To fabricate membranes of controlled thickness, we have used inexpensive and reproducible in situ depth rulers [38]. We typically produce membranes that are 10–20 μm thick, and thin them during tip production to 5–10 μm. After further thinning occurring during the process of making tips, the cantilever support beams and the pads are ~5 μm thick.

3.1.3. Integrated sharp tips

We use direct fabrication to integrate a variety of tips shapes onto the probes. The process involves a controlled undercut of a small masking island, which in our case is 5 × 5 μm². The tip is formed when the etchant undercuts the island sufficiently to lift it off. We have three types of masks available—SiN, SiO₂ and photoresist, so we can use a variety of chemistries to produce tips. SiN is an excellent mask for KOH, SiO₂ is a very good mask for DRIE with

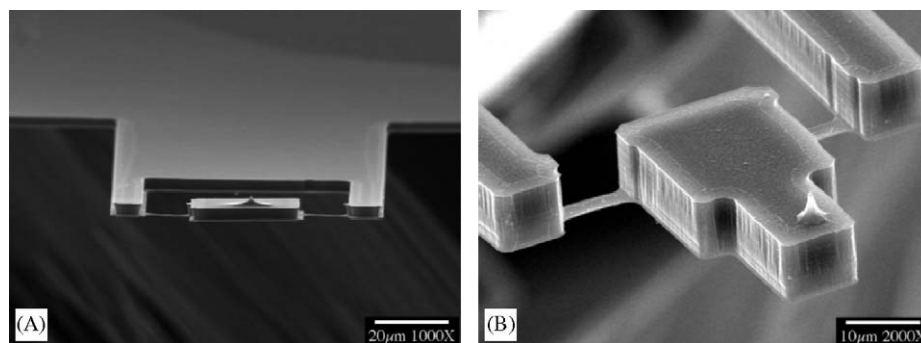


Fig. 5. Torsion levers for low-noise operation in liquid where viscous drag is high. (A) Symmetrically balanced torsion pad for low-force, contact mode, imaging and force spectroscopy. (B) Asymmetric torsion pad for tapping mode.

SF₆ and photoresist may be used to mask SF₆ and CF₄ RIE. We have used SF₆ to produce high-aspect atomically sharp tips (Fig. 3A and B). The undercut of a SiN mask by KOH produces octagonal tips with broad bases, four-fold symmetry and atomically flat walls (Fig. 3C and D). Tips directly fabricated in KOH have low aspect ratio = height/width = 1.2 and a cone angle of about 70°. These tips are not well suited for imaging high aspect ratio structures, but they have well-defined shapes and they can be used with soft biological materials. We have been able to produce taller tips by pre-etching a small post using DRIE prior to release by SF₆ and KOH [8,11,29]. Tips may be further sharpened by oxidation [39,40] without additional processing if dry SiO₂ is grown during the following steps.

3.1.4. Thin hinges

We deposit the hinge layer as a SiO₂/SiN LPCVD stack with the intent of using the SiN layer for the hinges and SiO₂ layer for protection. The thickness of the nitride layer is critical in defining the hinge stiffness. We have experimented with SiN thicknesses of 10–400 nm. A SiO₂ thickness of 100 nm has proven adequate to protect the hinge during processing (Fig. 4).

Both the thin films bear intrinsic mechanical stress (tensile for nitride and compressive for oxide) [13,41]. Due to the symmetric design of the hinges, we have not seen the stress-induced curvature that plagues asymmetrically supported cantilevers [14]. While the SiN/SiO₂ hinges may be used as is, we often soften them further with a short HF etch to remove the SiO₂. Since etch selectivity for oxide over nitride increases with decreasing HF concentrations [42], we use an aqueous mixture of 20% HF in 40% EtOH and 40% H₂O. Ethanol is added to the mixture to reduce surface tension. At this concentration of HF, the selectivity for SiO₂ to SiN is 100 to 1 [43], and the oxide layer is etched within seconds, while the nitride layer is stable for minutes.

3.1.5. Metal coatings

We have deposited metal layers on the pad both to increase reflectivity and to create magnetically sensitive levers. To correct for the low reflectivity of silicon (~30%) to the red light [44] typical of lasers used in AFM, we have deposited Au on the backside of the pad. A 50 nm Au layer is sufficient to achieve ~90% reflectivity. While Au coatings create a thermal bimorph which warps asymmetric cantilevers, our symmetric design with a rigid pad is immune to this effect.

3.2. A family of torsion probes

The torsional arrangement is advantageous for several reasons. During fabrication, the symmetry of the hinges prevents warping. In operation, despite the ultra-thin hinges, the levers are stable during transfer across air/liquid interface. The small area of the pads minimizes drag, increases the frequency response and decreases the low-frequency noise. Finally, orthogonally oriented hinges

allow the clean definition of two of the degrees of freedom and simplify the definition of resonant properties.

3.2.1. Small, fast and soft torsion AFM cantilevers

The basic unit in our family of probes is the torsion lever shown in Fig. 5. As described, the probe is small, compliant

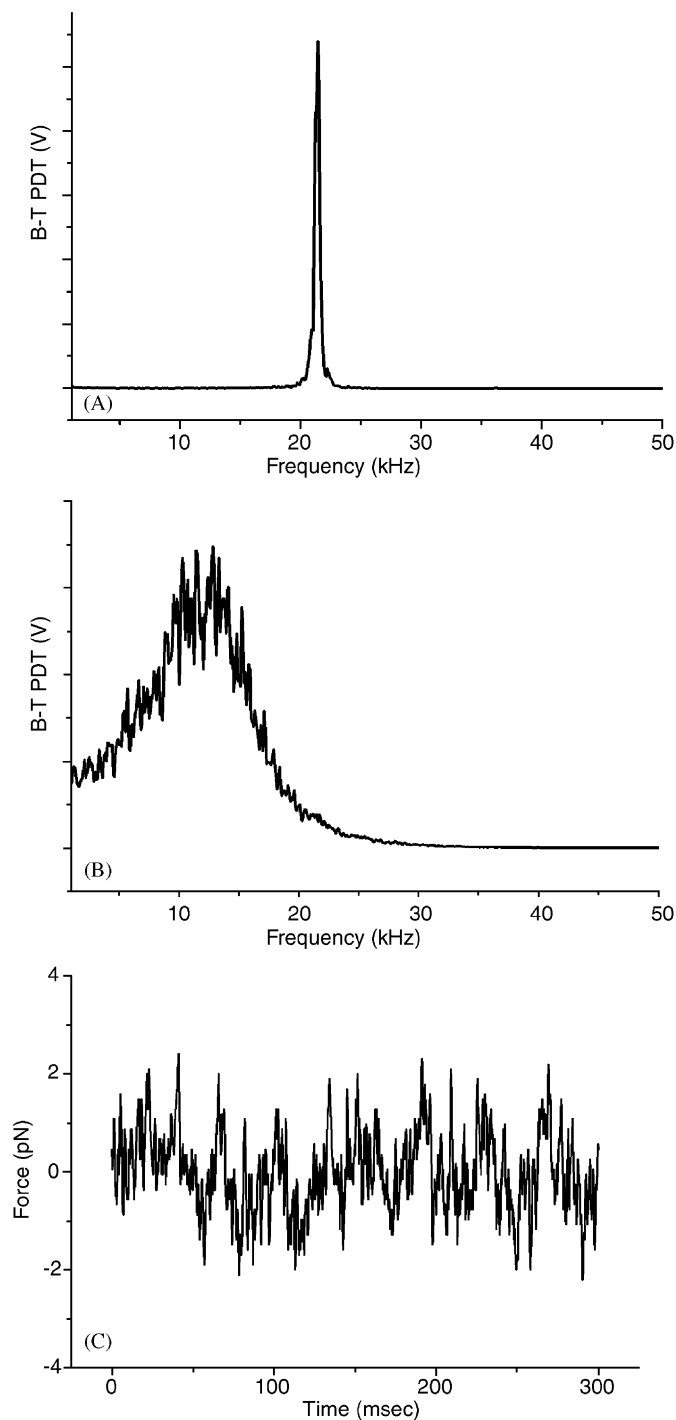


Fig. 6. Dynamic properties of a typical symmetric soft torsion lever ($20 \times 20 \times 5 \mu\text{m}^3$ pad on $10 \mu\text{m}$ long, $3 \mu\text{m}$ wide, 100-nm-thick hinges, $k = 0.009 \text{ N/m}$). (A) Resonant frequency in air ($f_0 = 21 \text{ kHz}$, $Q = 53$). (B) Resonant frequency in water ($f_0 = 12 \text{ kHz}$, $Q = 2.2$). (C) Torsion lever noise in water in a 1 kHz band ($F_{\text{rms}} = 0.82 \text{ pN}$).

and retains a high resonant frequency in water (Fig. 6). The levers are extended from the handle chip by a 150- μm -long extension beam. This distance is roughly the length of traditional cantilevers and provides sufficient clearance on standard microscopes.

We sized the pad to accept the typical (20 μm) optical beam waist of commercial AFMs. Our process allows further minimization, limited only by the optical resolution of contact photolithography, $\sim 0.5 \mu\text{m}$. An additional factor in determining the pad length is the optical gain—

shorter pads have higher gains ($\theta \approx 1/l$) [16]. Thus, shorter probes may be made stiffer and still retain high sensitivity.

The hinges are the major determinant of mechanical properties of the lever. Using $\sim 50\text{-nm}$ -thick hinges, we can reliably build probes softer than the softest commercially available AFM cantilevers ($\sim 0.01 \text{ N/m}$) and with resonances in water above 10 kHz (Fig. 6B).

These probes increase sensitivity, decrease noise and allow faster operation in all AFM operational modes [45]. Symmetric pads with minimum area and moment of inertia

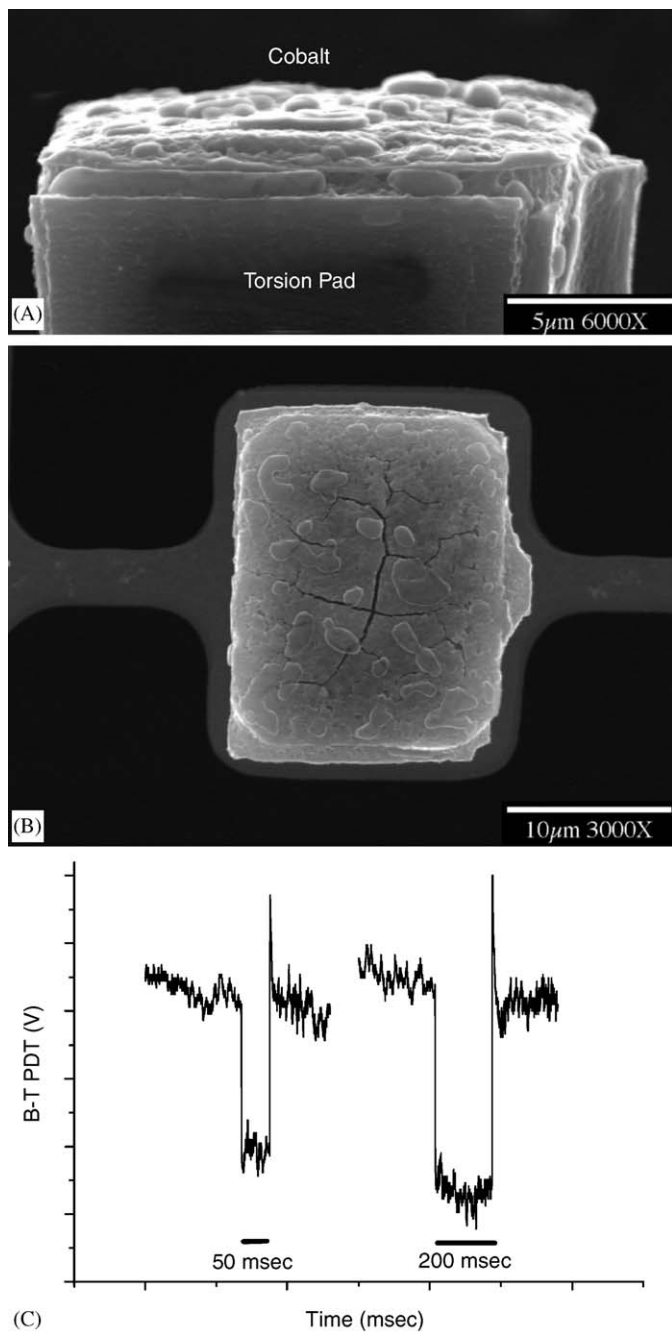


Fig. 7. Magnetically driven pad. (A) Side view and (B) top view, 100 nm cobalt layer deposited onto the topside of the torsion pad. (C) Actuation of the pad via a small non-calibrated electromagnet.

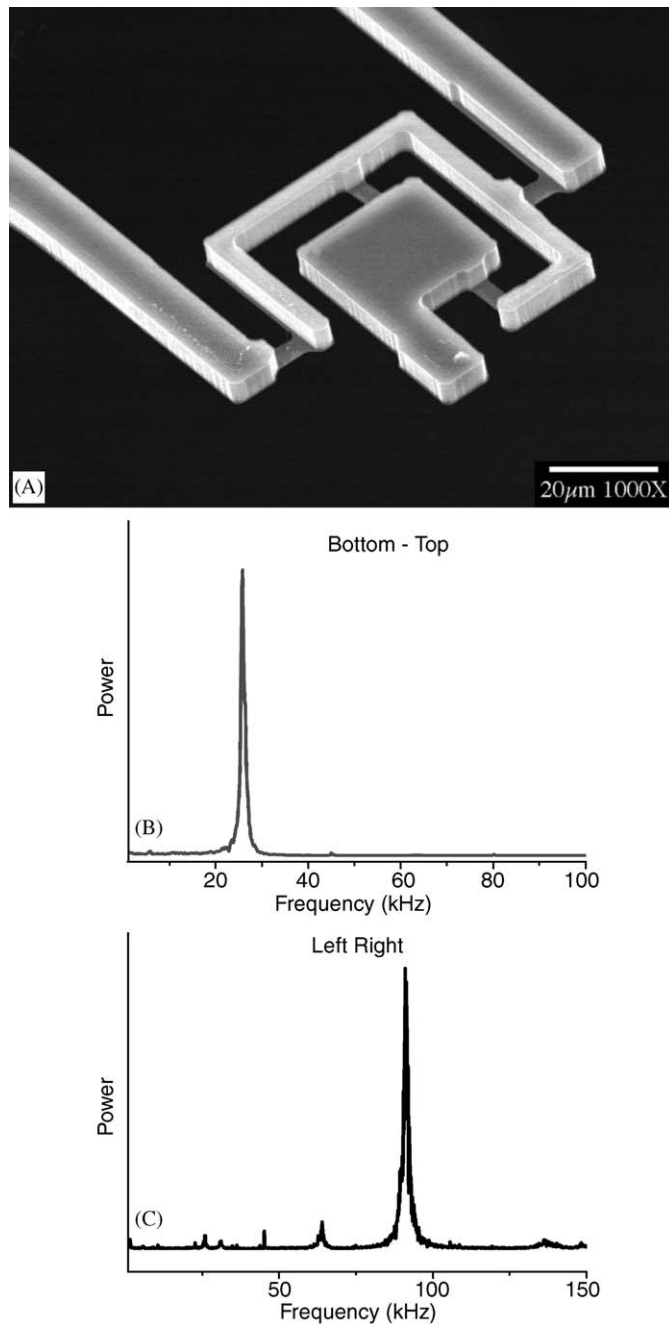


Fig. 8. Gimbaled frictional probes with two independent axes. (A) SEM of a probe with soft Si₃N₄ hinges. (B) Resonant peak in air (26 kHz) of the outer gimbal using the on B-T signal. (C) Resonant peak of the inner hinges (95 kHz) using the L-R signal.

have the highest resonant frequencies and Q -factors. These allow low noise recording (Fig. 6C) in open-loop force spectroscopy, closed-loop contact mode and frequency modulation imaging [46]. On the other hand, asymmetric pads (Fig. 5B) may be required to efficiently couple to external drive for tapping mode.

3.2.2. Magnetic drive

For dynamic studies using traditional methods, moving the cantilever requires moving the entire cantilever support structure with the scanning piezo [47] or moving the substrate [48]. This results in parasitic vibrations that interfere with the measurements. A much more ideal solution would be move only the cantilever pad itself. A first approximation of this mode was done by Lindsay's lab [32] and is currently available from Molecular Imaging. A standard cantilever is coated with a magnetostrictive layer and this magnetic bimorph is wiggled using an external field (MAC mode AFM). However, as with all asymmetric levers, inhomogeneities cause warping and drift. The torsion lever, with its small rigid pad, is a more ideal structure for magnetic drive. We can coat either the backside or the topside of the pad with ferromagnetic materials such as Co. On the backside, we deposit a conformal layer, covering the pads as well as the hinges. On the topside, we can control the geometry and deposit the magnet only onto the pad (Fig. 7A and B). If the coating is a hard magnetic material, it can be magnetized parallel to the pad and torqued by a normal B field [32] (Fig. 7C). A

soft magnetic coating can be torqued by a B field at an angle. The magnetic coatings can be applied in vacuum after fabrication with no additional masking necessary since a small amount of metal on the torsion hinges does not significantly affect the stiffness. Calculations suggest that with 100 nm coatings, 1 kG fields can apply 100 pN forces to the tip. The magnetic drive is also well suited to drive tapping mode and FM modulation [46].

3.2.3. Dual axis (gimbaled) levers

We have made levers with two independent deflection axes; a pad mounted on two sets of orthogonal springs arranged as a gimbaled mount (Figs. 8A, 9B and C). These levers provide several novel capabilities for the AFM:

- They can be used as exquisitely sensitive vectorial friction probes, especially with tall tips, by locating the tip where the hinge axes cross.
- With the tip located off the hinge centers, displacement of the two axes can be correlated to remove noise that does not arise from z -axis displacements.
- Self-referencing levers that remove drift.

Excess noise in the AFM comes from instrumental drift and environmental mechanical noise. If one could measure the sample displacement relative to the substrate rather than the laboratory reference frame, nearly all the excess noise would be removed. Hoerber's group [49] showed that by using two separate levers, one touching the sample and

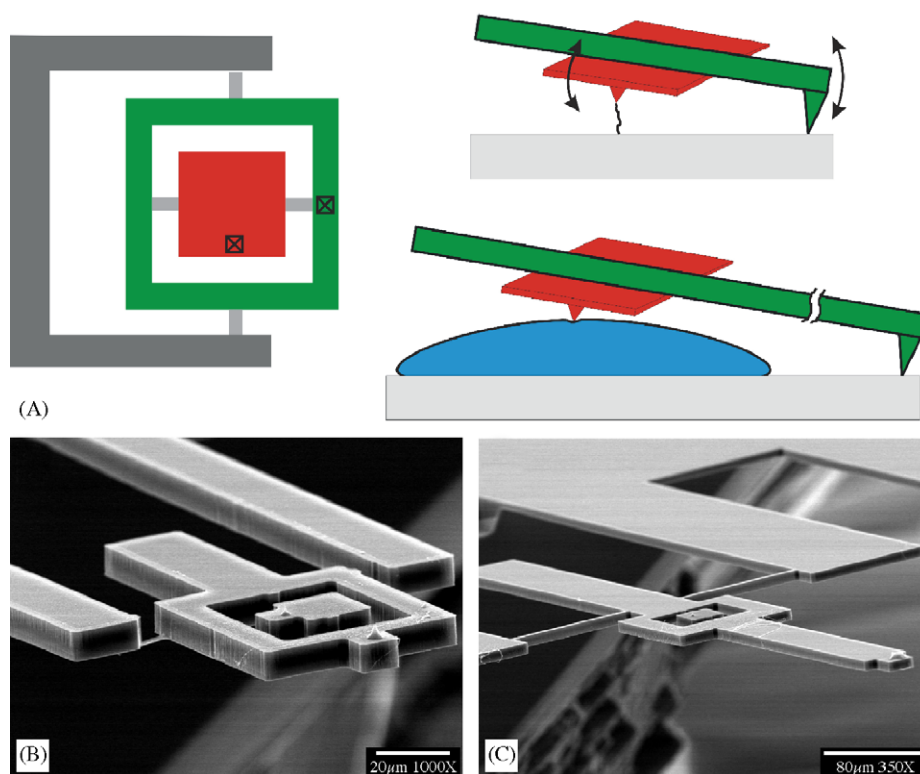


Fig. 9. Self-referencing AFM probes. (A) Cartoon of self-referencing probe. (B) Cartoon of probe used for self-referencing single molecule spectroscopy. (C) Self-referencing AFM cell surface probe with a long reference beam for increased clearance of the sample tip from the substrate.

one touching the substrate, they could easily achieve pN force resolution. However, their technique is experimentally cumbersome, involving two separate optical levers in a custom AFM.

Our dual axis lever accomplishes the same task with a single optical lever. The normal laser beam illuminates the mirror, but the two orthogonal axes can be decoded by the PDT (Bottom–Top, Left–Right). z -axis noise at higher frequencies is also removed by taking the difference of the two signals (after appropriate scaling for differences in optical gain of the two axes). Intensity fluctuations of the laser system can also be suppressed.

Fig. 8A shows a two-axis probe. Each of the vibration modes shows up in the orthogonal direction on the PDT. Flexing of the outer gimbal shows up at 26 kHz on the bottom–top (B–T) PDT channel (Fig. 8B). The inner pad has a 95 kHz resonant peak on the left–right (L–R) channel (Fig. 8C). The resonant frequency and spring constant of the inner pad may be engineered in the same way as for the torsion probes that we discussed above. This probe may be used for simultaneous friction and topography imaging.

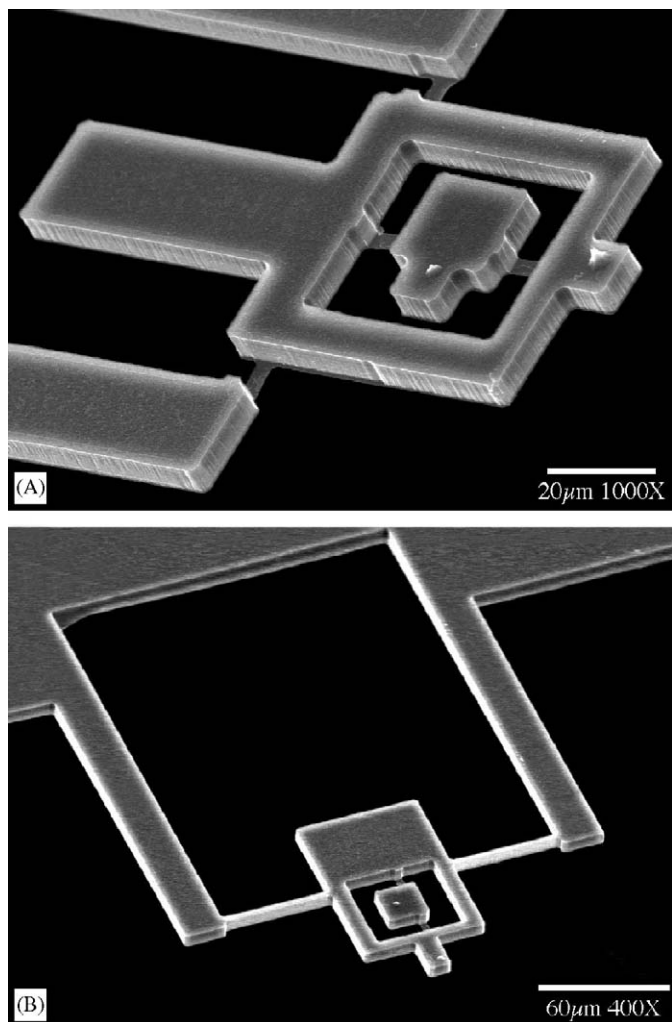


Fig. 10. SEM images of reference levers. (A) Soft reference lever. (B) Stiff reference lever on the same wafer using Si hinges.

Another application of this probe is for resolution of the angle between a tip-linked polymer and the z -axis of the AFM, a situation typical in dynamic force spectroscopy. Off-normal angles cause underestimation of sample stiffness since only the z component is measured. With high compliance springs and at small angles, the deflection angle of the pad will tend to become normal to axis of the polymer. By using feedback to minimize the tipping angle, the tension axis can be made normal to the substrate [50].

In another variation of the gimbaled probe, each orthogonal axis has its own tip, one of which contacts the sample and the other the substrate. Lever and tip geometries can be varied depending upon the experiment (Fig. 9A). To examine the surface of cells, for example, the reference tip should be placed far from the sample tip to allow the sample tip clearance above the cell (Fig. 9C). For increased detail resolution, the two tips can be placed close together to create a differential contrast image of topology or compliance (Fig. 9B). For single molecule force spectroscopy, the dual axis lever provides not only improved high-frequency response but also improved low-frequency response by removing drift.

Our process allows simultaneous production of soft hinges for the measurement levers and either soft SiN or hard Si hinges for the reference levers. Soft reference hinges (Fig. 10A) maximize force sensitivity while stiff hinges (Fig. 10B) allow more stable reference contact and maximum noise reduction.

4. Conclusion

We have developed a microfabrication process suitable for mass production of torsion levers with a wide variety of geometries and mechanical properties. On a single die, we can place multiple levers of the same or different size with a wide variety of spring constants. These levers are a significant advance in several areas: composite design, no warping, reduced drag, increased frequency resolution, lower noise and orthogonal sensitivity. The levers have moving areas that need only be as big as the mirror required for the optical lever. Minimal area results in optimal performance in liquids. While this paper has focused on applications of the technology to AFM cantilever design, the same fabrication process can be applied to building sensors for multi-axis accelerometers, gyroscopes, movable mirrors, switches, magnetometers, oscillators and other sensors.

Acknowledgments

Microfabrication was done at the Cornell NanoScale Facility, Ithaca, New York. This work was supported by NIH R01 GM060648.

References

- [1] G. Binnig, C.F. Quate, C. Gerber, Phys. Rev. Lett. 56 (1986) 930.
- [2] G. Meyer, N.M. Amer, Appl. Phys. Lett. 53 (1988) 1045.

- [3] J.B. Thompson, B. Drake, J.H. Kindt, J. Hoskins, P.K. Hansma, *Nanotechnology* 12 (2001) 394.
- [4] F. Atamny, A. Baiker, *Surf. Sci.* 323 (1995) L314.
- [5] F. Gittes, C.F. Schmidt, *Eur. Biophys. J.* 27 (1998) 75.
- [6] H.-J. Butt, P. Siedle, K. Seifert, K. Fendler, T. Seeger, E. Bamberg, A.L. Weisenhorn, K. Goldie, A. Engel, *J. Microsc.* 169 (1993) 75.
- [7] L.D. Landau, E.M. Lifshitz, *Course of theoretical physics. Fluid Mechanics*, vol. 6, Pergamon Press, Oxford, 1959.
- [8] T.R. Albrecht, S. Akamine, T.E. Carver, C.F. Quate, *J. Vac. Sci. Technol. A* 8 (1990) 3386.
- [9] M. Tortonese, *IEEE Eng. Med. Biol. Mag.* 16 (1997) 28.
- [10] T. Aoki, M. Hiroshima, K. Kitamura, M. Tokunaga, T. Yanagida, *Ultramicroscopy* 70 (1997) 45.
- [11] J. Brugger, R.A. Buser, N.F. de Rooij, *Sensor Actuator Phys.* 34 (1992) 193.
- [12] R.J. Grow, S.C. Minne, S.R. Manalis, C.F. Quate, *J. Microelectromech. Syst.* 11 (2002) 317.
- [13] S. Habermehl, *J. Appl. Phys.* 83 (1998) 4672.
- [14] L.A. Wenzler, G.L. Moyes, T.P. Beebe, *Rev. Sci. Instrum.* 67 (1996) 4191.
- [15] M.B. Viani, T.E. Schaffer, A. Chand, M. Rief, H.E. Gaub, P.K. Hansma, *J. Appl. Phys.* 86 (1996) 2258.
- [16] D.A. Walters, J.P. Cleveland, N.H. Thomson, P.K. Hansma, M.A. Wendman, G. Gurley, V. Elings, *Rev. Sci. Instrum.* 67 (1996) 3583.
- [17] A. Chand, M.B. Viani, T.E. Schaffer, P.K. Hansma, *J. Microelectromech. Syst.* 9 (2000) 112.
- [18] M.B. Viani, T.E. Schaffer, G.T. Paloczi, L.I. Pietrasana, B.L. Smith, J.B. Thompson, M. Richter, M. Rief, H.E. Gaub, K.W. Plaxco, A.N. Cleland, H.G. Hansma, P.K. Hansma, *Rev. Sci. Instrum.* 70 (1999) 4300.
- [19] M.B. Viani, T.E. Schaffer, A. Chand, M. Rief, H.E. Gaub, P.K. Hansma, *J. Appl. Phys.* 86 (1999) 2258.
- [20] P.C. Zhang, A.M. Keleshian, F. Sachs, *Nature* 413 (2001) 428.
- [21] M.G.L. Gustafsson, J. Clarke, *J. Appl. Phys.* 76 (1994) 171.
- [22] S.A. Miller, K.L. Turner, N.C. MacDonanld, *Rev. Sci. Instrum.* 68 (1997) 4155.
- [23] S. Evoy, D.W. Carr, L. Sekaric, A. Olkhovetz, J.M. Parpia, H.G. Craighead, *J. Appl. Phys.* 86 (1999) 6072.
- [24] Z.Q. Peng, P. West, *Appl. Phys. Lett.* 86 (2005) 014107-1.
- [25] N. Lobontiu, E. Garcia, S. Canfield, *Smart Mater. Struct.* 13 (2004) 12.
- [26] H.B. Chan, V.A. Aksyuk, R.N. Kleiman, D.J. Bishop, F. Capasso, *Science* 291 (2001) 1941.
- [27] A. Beyder, C. Spagnoli, F. Sachs, in preparation.
- [28] J.M. Olson, *Mater. Sci. Semicond. Process.* 5 (2002) 51.
- [29] A. Boisen, O. Hansen, S. Bouwstra, *J. Micromech. Microeng.* 6 (1996) 58.
- [30] J. Itoh, Y. Tohma, S. Kinemaru, K. Shimizu, *J. Vac. Sci. Technol. B* 13 (1995) 331.
- [31] F. Laermer, A. Urban, *Microelectron. Eng.* 67-8 (2003) 349.
- [32] W.H. Han, S.M. Lindsay, *Appl. Phys. Lett.* 69 (1996) 4111.
- [33] N.A. Burnham, X. Chen, C.S. Hodges, G.A. Matei, E.J. Thoreson, C.J. Roberts, M.C. Davies, S.J. Tendler, *Nanotechnology* 14 (2003) 1.
- [34] J.L. Hutter, J. Bechhoefer, *Rev. Sci. Instrum.* 64 (1993) 1868.
- [35] S. Besch, K. Snyder, P.C. Zhang, F. Sachs, *Cell Biochem. Biophys.* 39 (2003) 195.
- [36] W.T. Chang Chien, C.O. Chang, Y.C. Lo, Z.W. Li, C.S. Chou, *J. Micromech. Microeng.* 15 (2005) 833.
- [37] X.-P. Wu, W.H. Ko, *Sensor Actuator* 18 (1989) 207.
- [38] P.-Z. Chang, L.-J. Yang, *J. Micromech. Microeng.* 8 (1998) 182.
- [39] R.B. Marcus, T.T. Sheng, *J. Electrochem. Soc.* 129 (1982) 1278.
- [40] R.B. Marcus, T.S. Ravi, T. Gmitter, K. Chin, D. Liu, W.J. Orvis, D.R. Ciarlo, C.E. Hunt, J. Trujillo, *Appl. Phys. Lett.* 56 (1990) 236.
- [41] M. Maeda, M. Itsumi, *Phys. B Condens. Matter* 324 (2002) 167.
- [42] J.L. Vossen, W. Kern, *Thin Film Processes*, Academic Press, New York, 1978.
- [43] K.R. Williams, R. Muler, *J. Microelectromech. Syst.* 5 (1996) 256.
- [44] C.-R. Yang, P.-Y. Chen, Y.-C. Chiou, R.-T. Lee, *Sensor Actuator Phys.* 119 (2005) 263.
- [45] A. Beyder, F. Sachs, in preparation.
- [46] T. Fukuma, K. Kobayashi, K. Matsushige, H. Yamada, *Appl. Phys. Lett.* 86 (2005) 193108-1.
- [47] N. Jalili, K. Laxminarayana, *Mechatronics* 14 (2004) 907.
- [48] I. Revenko, R. Proksch, *J. Appl. Phys.* 87 (2000) 526.
- [49] S.M. Altmann, P.-F. Lenne, J.K.H. Horber, *Rev. Sci. Instrum.* 72 (2001) 142.
- [50] S. Besch, A. Beyder, F. Sachs, in preparation.